On Coupled Solid-Fluid Problems for Cohesionless Soils

W. Ehlers
Prof. Dr.-Ing.
Institut für Mechanik (Bauwesen), Universität Stuttgart, Germany
H. Müllerschön
Dipl.-Ing.
Institut für Mechanik (Bauwesen), Universität Stuttgart, Germany

Summary The present paper outlines the stress-strain behaviour of cohesionless soils under saturated and unsaturated (empty) conditions by the example of dense Berlin Sand. Sand as well as soils in general are porous media consisting of a soil skeleton with filled or empty voids. To describe strains and flow processes in such a porous solid, an elasto-plastic model is used and presented in the framework of the Theory of Porous Media (TPM) defined by the elements mixture theory and concept of volume fractions. Within the constitutive equations of the elasto-plastic model, the elastic response is described by a materially non-linear elasticity law. Plastic deformations are considered in the context of a single-surface yield function with isotropic hardening properties. Non-associated flow is realized with an additional plastic potential function. Isotropic behaviour is assumed and the study is restricted to small strains. Parameter identification for the described model is shown for dense Berlin Sand on the basis of triaxial tests. The presented model is implemented into the finite element code PANDAS,* numerical examples will demonstrate the capability of the formulation.

1. INTRODUCTION

A soil structure consists of an assemblage of particles with different sizes and shapes which form a skeleton whose voids are either empty or filled with a pore-fluid. The stresses carried by the soil skeleton are conventionally termed *effective stresses* in the soil mechanics literature (Terzaghi, 1943), and those in the fluid are called *pore-fluid pressure*. In the case in which flow of the pore-fluid takes place, there is an interaction between the skeleton deformation and the pore-fluid flow. Therefore, the solution of this problem requires a multiphase continuum formulation. Such a formulation can be carried out by use of the well-founded framework of the Theory of Porous Media (TPM). The TPM approach is based on a homogenization process to handle the microscopically inhomogeneous porous solid material with a macroscopic continuum mechanical description, *cf.* e. g. the work by Truesdell & Toupin (1960), Bowen (1976, 1980), de Boer & Ehlers (1990), de Boer *et al.* (1991) and Ehlers (1993).

To describe the stress-strain relation of a granular soil matrix, an elasto-plastic model seems to be suitable. Basis of an elasto-plastic theory is the assumption that the total deformation consists of the sum of a recoverable elastic part and an irreversible plastic part. Isolation of the elastic deformation part from the total deformation within triaxial experiments is possible through moderate unload-reload stress-paths, where only recoverable strains occur. Furthermore, experimental results indicate that the elastic parameters, as e. g. the shear modulus or the Young's modulus, are functions of the stress state, respectively of the deformation of the structure. Nevertheless, a thermodynamically consistent elasticity law can be formulated without any restriction to the existence of a hyperelastic potential (Loret, 1985). Plastic strains are described within a rate-independent plasticity approach. The presented contribution proceeds from a single-surface yield function, a non-associated flow rule based on an additional plastic potential function and an isotropic work-hardening formulation. The evolution of the yield surface is defined by rate equations for two parameters included in the yield criterion. In this paper, the formulation of the yield condition is shown for cohesionless materials. However, the general plasticity model is not restricted to cohesionless soils. Although the model is rather complex, the included parameters can be identified on the basis of the results of conventional triaxial compression and extension tests. Evaluation of experimental results and parameter identification is shown in the present paper.

For the numerical treatment of the problem within the finite element method (FEM), the weak formulation of the field equations is used. The elasto-plastic model is implemented in the numerical code PANDAS to calculate the stress-strain relations of the soil matrix under saturated and empty conditions. Finally, the capability of the model is demonstrated by numerical examples.

*Porous media Adaptive Nonlinear finite element solver based on Differential Algebraic Systems

2. THEORY OF POROUS MEDIA

The description of coupled deformation-flow processes in porous materials requires the consideration of a multi phase problem within the Theory of Porous Media proceeding from the classical mixture theory and the concept of volume fractions.

In the following, a materially incompressible two-phase model is considered. Thereby, the constituents φ^α are a solid phase ($\alpha = S$), described through an elasto-plastic model, and a viscous fluid phase ($\alpha = F$). The inclusion of material incompressibility of a constituent implies incompressibility in the material's micro range, which does not lead to macroscopic incompressibility. Thus, even if the realistic density $\rho^{\alpha R}$ of a constituent φ^α is constant, the partial density $\rho^\alpha = n^\alpha \rho^{\alpha R}$ can still change through a change of the volume fraction n^α.

The model incorporates three independent fields, the solid displacement $\mathbf{u}_S$, the seepage velocity $\mathbf{w}_F$ and the effective fluid pressure p. The corresponding three equations for quasi-static considerations (negligible accelerations),

$$-\frac{k^F}{\gamma^{FR}}(\operatorname{grad} p - \rho^{FR}\,\mathbf{b}) - n^F\,\mathbf{w}_F = \mathbf{0} \quad (1)$$

$$\operatorname{div}(\mathbf{T}_E^S - p\,\mathbf{I}) + (n^S\rho^{SR} + n^F\rho^{FR})\,\mathbf{b} = \mathbf{0} \quad (2)$$

$$\operatorname{div}\left[(\mathbf{u}_S)_S^{'} + n^F\,\mathbf{w}_F\right] = 0 \quad (3)$$

can be obtained from the kinematics, the balance relations and the constitutive equations described in Ehlers (1993) and Diebels *et al.* (1998). Therein, k^F is the Darcy permeability parameter, $\mathbf{b}$ the body force (gravity), γ^{FR} the effective specific weight and $(\mathbf{u}_S)_S^{'}$ the time derivative of the solid motion. The solid extra stress tensor $\mathbf{T}_E^S$ represents the effective stress of the soil matrix. Equation (1) represents Darcy's law describing the internal friction between the skeleton and the viscous pore-fluid.

Unsaturated (empty) conditions are given for $k^F = \infty$ relative to the rate of loading, no excess pore-fluid pressure over atmospheric pressure builds up.

3. ELASTO-PLASTIC MODEL

3.1 A New Formulation of An Elasticity Law

As mentioned above elastic strains can be isolated through unload-reload cycles in triaxial tests. In case of moderate unloading, hysteresis effects can be neglected and intermittent strains are assumed to be entirely recoverable and hence elastic (Figure 1). A special property of granular materials is the dependence of the elastic stiffness on the stress state, respectively on the deformation state of the structure. To take into account this phenomenon, the elastic parameters vary with the elastic volumetric strain, and furthermore consider the plastic volumetric strain and the point of compaction as governing parameters.

In particular, hydrostatic tests show a non-linear behaviour towards the point of compaction, compare Figure 2, defined by a critical packing density, where an increase of the isotropic load cannot cause a further increase of the volumetric strains, unless there is grain crunching.

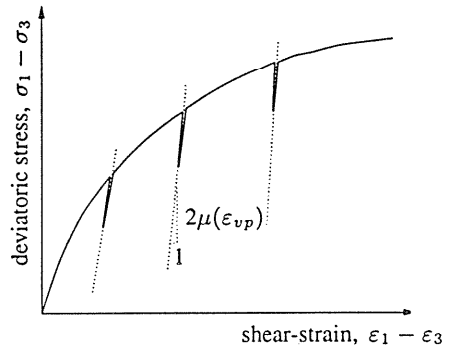

Figure 1. Unload-reload cycles in triaxial compression test, $\sigma_3 = \text{const.}$ (qualitatively)

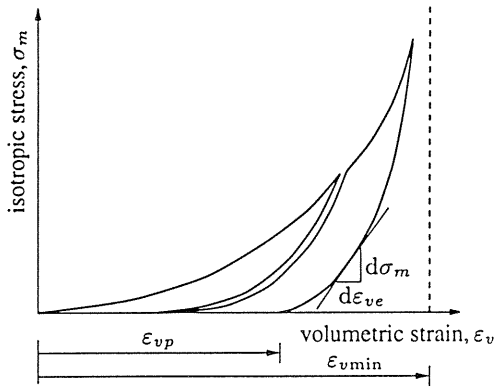

Figure 2. Unload-reload cycles in isotropic compression test (qualitatively).

To describe the elastic behaviour, it is assumed that

$$\mathbf{T}_E^S = 2\mu\,\boldsymbol{\varepsilon}_e^D + k\,(\boldsymbol{\varepsilon}_e \cdot \mathbf{I})\mathbf{I} \quad (4)$$

be a modification of Hooke's law. The tensor $\boldsymbol{\varepsilon}_e^D = \boldsymbol{\varepsilon}_e - \frac{1}{3}(\boldsymbol{\varepsilon}_e \cdot \mathbf{I})\mathbf{I}$ is the deviatoric part of the elastic strain tensor $\boldsymbol{\varepsilon}_e$. To consider the variation of the shear strength, the shear modulus μ is introduced as a linear function of the plastic volumetric strain $\varepsilon_{vp} = \boldsymbol{\varepsilon}_p \cdot \mathbf{I}$:

$$\mu = \mu(\varepsilon_{vp}) = \mu_0\,|\varepsilon_{vp}| \quad (5)$$

Therein, ε_{vp} must be understand as a parameter and thus, μ is a constant at any given state of the plastic deformation.

The volumetric plastic strain ε_{vp}, according to

a unload-reload loop and therefore to a special value of μ, is determined with results of triaxial compression tests carried out on Berlin Sand. Stress paths of these axial compression tests lead to a point where unload-reload is applied and consist of two parts: isotropic compression up to an arbitrary confining pressure and further, increase of deviatoric stress up to the specified point. Thus, ε_{vp} can be split into ε_{vp}^{hyd} and ε_{vp}^{dev}.

Completely unloading from a choosen isotropic confining pressure state leads to remaining volumetric strain. This strain is assumed to be the plastic part ε_{vp}^{hyd} of the total strain assigned to this hydrostatic stress state.

Within the increase of the axial stress, respectively of the deviatoric stress, there is still an increase of volume contraction. The corresponding volumetric strain ε_{vp}^{dev} is determined through extension of the considered unload-reload cycle as it is shown in Figure 3.

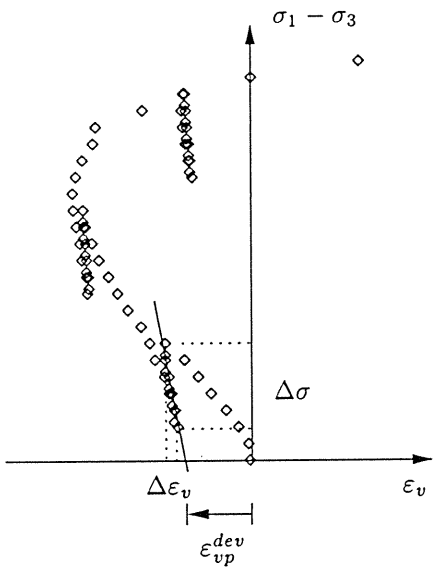

Figure 3. Determination of the volumetric plastic strain ε_{vp}^{dev} for a particular unload-reload cycle in a triaxial compression test ($\sigma_3 = -100$ kN/m^2).

Therewith, it is possible to assign to every unload-reload loop and hence to every value of the shear modulus an according total volumetric plastic strain

$$\varepsilon_{vp} = \varepsilon_{vp}^{hyd} + \varepsilon_{vp}^{dev} \tag{6}$$

This assignment is plotted in Figure 4 for a few triaxial compression tests ($\sigma_3 = -50, -100, -200, -350, -500$ and -750 kN/m^2) with several unload-reload cycles.

The bulk modulus k not only depends on ε_{vp} as a parameter of the plastic deformation, but is also a function of the elastic volumetric strains $\varepsilon_{ve} = \varepsilon_e \cdot \mathbf{I}$. Finally, the point of compaction must be included by

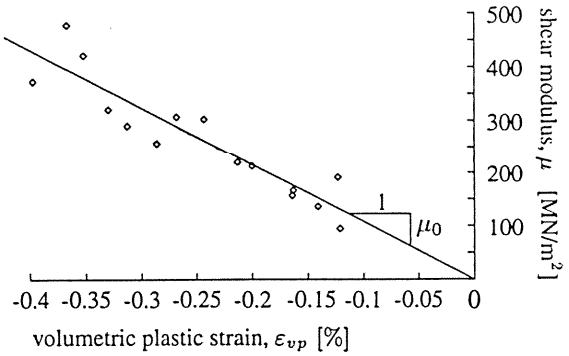

Figure 4. Observed shear modulus for different values of volumetric plastic strain, approximated by a linear function $\mu(\varepsilon_{vp}) = \mu_0 \varepsilon_{vp}$.

the parameter $\varepsilon_{v\,\min}$ describing the maximum of the volume contraction. Thus,

$$\begin{aligned} k &= k\,(\varepsilon_{ve}; \varepsilon_{vp}, \varepsilon_{v\,\min}) \\ &= k_1 + k_2 \ln\left[1 + \varepsilon_{ve}\,(\varepsilon_{ve} + \varepsilon_{vp} - \right. \\ &\quad \left. - \varepsilon_{v\,\min} + \frac{1}{\varepsilon_{vp} - \varepsilon_{v\,\min}}\,)\right] \varepsilon_{ve} \end{aligned} \tag{7}$$

k_1 and k_2 are constants to be fitted at unload-reload cycles in isotropic compression tests. Parameters for the considered dense Berlin Sand are given in Section 4, Table 1.

3.2 Plastic Soil Properties

3.2.1 Constitutive equations

In order to bound the elastic domain, a *single-surface yield function* (Ehlers, 1995) exhibiting a closed and smooth shape in the principal stress space is introduced:

$$\begin{aligned} F(\mathbf{T}_E^S, q^d, q^h) &= \sqrt{\Gamma\,\mathrm{II}_D + \tfrac{1}{2}\alpha \mathrm{I}^2 + \delta^2 \mathrm{I}^4} + \\ &\quad + \beta \mathrm{I} + \epsilon \mathrm{I}^2 - \kappa = 0 \end{aligned} \tag{8}$$

$$\Gamma(\mathbf{T}_E^S, q^d) = \left(1 + \gamma\,\mathrm{III}_D / (\mathrm{II}_D)^{3/2}\right)^m$$

The first invariant I and the deviatoric second and third invariants $\mathrm{II}_D, \mathrm{III}_D$ of the extra stress tensor $\mathbf{T}_E^S$ characterize the stress state in equation (8). The function $\Gamma(\mathbf{T}_E^S, q^d)$ with the deviatoric parameters

$$q^d = (\gamma, m)^T \tag{9}$$

specify the shape of the yield-curve in the octahedral plane. The hydrostatic material parameters

$$q^h = (\alpha, \beta, \delta, \epsilon, \kappa)^T \tag{10}$$

govern the effect of *isotropic work-hardening* processes, realized through the rate equations

$$(q^h)'_S = C_i\,(\overset{\star}{q}{}^h - q^h)\,(W_p)'_S \tag{11}$$

with the boundary conditions

$$q^h(W_p = 0) = q_0^h > \overset{\star}{q}{}^h$$
$$q^h(W_p \to \infty) = q_\infty^h = \overset{\star}{q}{}^h \tag{12}$$

W_p is the plastic work per unit volume accumulated during the deformation process, C_i are constants to fit equation (11) to experimental results, q_0^h is the parameter set of the initial yield surface and $\overset{\star}{q}{}^h$ comprises the parameters of the limiting yield surface, respectively of the failure surface. Reformulation of equation (8) with the Reuss variables r (yield radius) and Θ (Lode angle) leads to

$$F(\mathrm{I}, \mathrm{II}_D, \mathrm{III}_D; q^d, q^h) \Rightarrow F(\mathrm{I}, r, \Theta; q^d, q^h) \tag{13}$$

Thus, the yield function can be given by

$$\begin{aligned} r(\Theta, \mathrm{I}) &= F_h(\mathrm{I})\, F_d(\Theta) \\ F_h(\mathrm{I}) &= \sqrt{2}\left[(\epsilon^2 - \delta^2)\,\mathrm{I}^4 + 2\beta\epsilon\mathrm{I}^3 + \right. \\ &\quad \left. + \left(\beta^2 - \tfrac{1}{2}\alpha - 2\epsilon\kappa\right)\mathrm{I}^2 - 2\beta\kappa\mathrm{I} + \kappa^2\right]^{1/2} \\ F_d(\Theta) &= \left[1 + \tfrac{2}{\sqrt{27}}\gamma\sin(3\Theta)\right]^{-m/2} \end{aligned} \tag{14}$$

Therein, $r(\Theta, \mathrm{I})$ is the yield radius given as the product of two independent functions, $F_h(\mathrm{I})$ and $F_d(\Theta)$, where $F_h(\mathrm{I})$ represents the hydrostatic shape function with $\Theta = 0°$, while $F_d(\Theta)$ describes the shape of the yield condition in the deviatoric plane.

In general, soils are frictional materials and the description of plastic flow requires a *non-associated flow rule*. Therefore, an additional plastic potential (Ehlers & Mahnkopf 1998)

$$G(\mathrm{T}_E^S, q^h, \psi_1, \psi_2) = \sqrt{\psi_1 \mathrm{II}_D + \tfrac{1}{2}\alpha\,\mathrm{I}^2 + \delta^2\,\mathrm{I}^4} + \\ + \psi_2\beta\,\mathrm{I} + \epsilon\,\mathrm{I}^2 \tag{15}$$

is defined. The parameters ψ_1 and ψ_2 specify the deviation of the shape of the plastic potential, respective of the shape of the yield surface in the hydrostatic plane. In the deviatoric plane, coaxial flow perpendicular to the hydrostatic axis is assumed. Given equation (15), the flow rule

$$(\epsilon_p)_S' = \Lambda\,\frac{\partial G}{\partial \mathrm{T}_E^S} \tag{16}$$

holds, where Λ is the usual plastic multiplier.

3.2.2 Deviatoric shape of the yield function

Cubical triaxial tests, performed for example by Yamada & Ishihara (1979), indicate that the deviatoric contours of the plastic work (equipotential surfaces of W_p) have circular shapes at low stress levels and gradually change into rounded triangular shapes when the stress level increases up to failure, compare Figure 5.

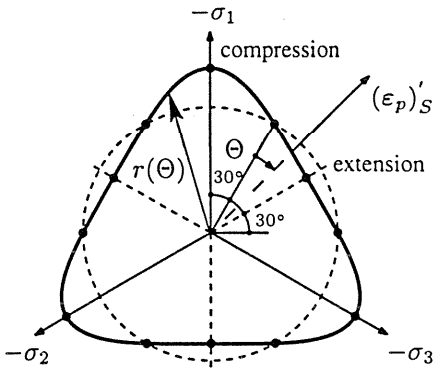

Figure 5. Octahedral plane; cross-section perpendicular to the hydrostatic axis.

The formulation of the yield function in (8) allows the description of this property for a suitable choice of γ and m. The ratio of the compression and the extension radii, r_c and r_e, in the failure state, provides the first condition for the determination of γ and m.

In addition, the restriction to convexity evaluated at the point of extension delivers the second condition for these parameters. Change of the shape of the yield curve is realized through a linear increase of γ from $\gamma = 0$ (circular) to γ_{max} (rounded triangular shape) according to the deviatoric stress level.

3.2.3 Hydrostatic shape of the yield function

In equation (14), F_h describes the contour of the yield curve in the hydrostatic plane for $\Theta = 0°$. The parameters q^h (10) specify the shape of the curve. For sand as a cohesionless material, κ and α are zero. Thus, there are three remaining parameters β, δ and ϵ to determine the yield criterion.

Since yielding is a continous process for frictional materials, there may not be a distinct point of initial yielding on a stress-strain curve. The determination of yield surfaces have been studied in detail since the plasticity theory has been found effective in modeling deformation of frictional materials. In the presented model, the method of identification of yield points and yield surfaces in stress space is based on the assumption that yield surfaces are equivalent to plastic work contours, as it was suggested by Lade & Kim (1988). For each stage of several triaxial compression tests and of an Isotropic compression test, the plastic work W_p is calculated. A family of yield contours is approximated through an optimization process to stress points with the same values of W_p, compare Figure 8.

The parameter β is directly connected to the slope of the yield surface at the origin of the stress space ($\mathrm{I} = 0$). Comparison with the friction angle ϕ of the well-known Mohr-Coulomb-theory leads to the relation $\beta = \frac{1}{3}\sin\phi$ for the failure state. The

evaluation of the friction angle ϕ for compression tests with six different values of the confining pressure is shown in Figure 6. An increase of the friction angle with a decrease of applied confining pressure is observed. For $I = 0$, $\phi = 48.6°$ is assumed, which corresponds to $\beta = 0.25$. During hardening and hence for the above mentioned optimization, β is kept constant at this value.

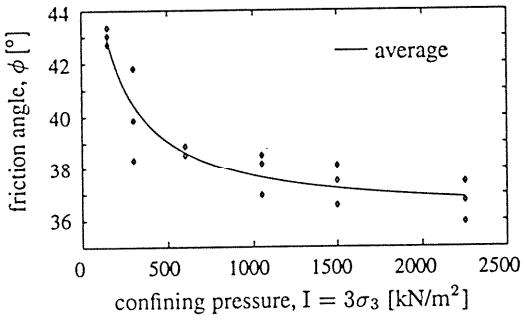

Figure 6. Observed friction angles *vs.* confining pressure for dense Berlin Sand.

Hence, δ and ϵ are the hardening parameters, which are evaluated according to the hardening law in equation (11). Figure 8 shows a choice of adapted yield curves for different values of W_p. Since there are two hardening parameters for the description of the hydrostatic yield function, a non-similar evolution of the shape of the yield curve is possible and therefore a more flexible fit to the experimental results is feasible.

A failure surface is enclosed in the model defined through $\overset{*}{\delta}$ and $\overset{*}{\epsilon}$, which are the limit values for the evolution of δ and ϵ, compare Figure 7. In hydrostatic direction, the expansion of the yield surface for sand is very sensitive, e. g. increments of volumetric plastic strains are rather small for high stress levels. In combination with the presented elasticity law in Section 3.1, the increments of total volumetric strains converge to very small values, which makes sense for granular materials. Following a triaxial compression stress path leads to a critical point of deviatoric stress level, where the yield surface no more expands and hence ideal plasticity takes place.

As mentioned above, non-associated flow can be realized through an additional plastic potential G (eq. (15)). The parameters ψ_1 and ψ_2 specify the projection of the flow direction in the hydrostatic plane. Determination of these parameters is done through a fit to volume change curves of triaxial compression tests.

4. PARAMETER VALUES FOR BERLIN SAND

Table 1 shows the parameter values for the presented elasto-plastic model determined in triaxial tests on dense Berlin sand. The characteristics of the sand are summerized as follows: coefficient of uniformity:

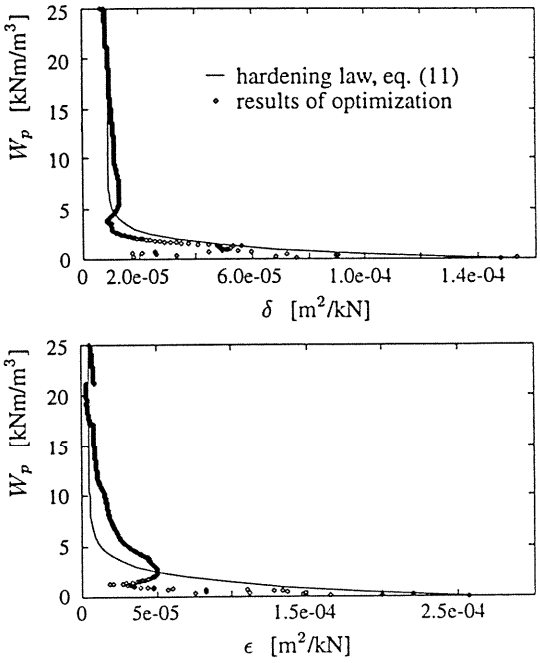

Figure 7. Development of the parameters δ and ϵ during hardening.

2.1; specific weight of grains: $\rho^{SR} = 2.653$ g/cm^3; maximum void ratio: 0.817; minimum void ratio: 0.481. All tests are realized on samples with a bulk density of $\rho_d = n_{0S}^S \rho^{SR} = 1.71$ g/cm^3. This density corresponds to an initial volume fraction of the solid of $n_{0S}^S = 0.644$.

Table 1. Determined material parameters of the elasto-plastic model for dense Berlin Sand.

Elasticity			
Parameter	Symbol	Value	Unit
Elasticity law	μ_0	$1.07 \cdot 10^8$	kN/m^2
	k_1	$3.86 \cdot 10^4$	kN/m^2
	k_2	$6.11 \cdot 10^6$	kN/m^2
	$\epsilon_{v\,\min}$	-0.019	–
Plasticity			
Yield and hardening functions	α	0	–
	κ	0	kN/m^2
	β	0.25	–
	$\overset{*}{\delta}$	$8.81 \cdot 10^{-6}$	m^2/kN
	C_δ	0.81	m^2/kN
	δ_o	$1.53 \cdot 10^{-4}$	m^2/kN
	$\overset{*}{\epsilon}$	$5.00 \cdot 10^{-6}$	m^2/kN
	C_ϵ	0.60	m^2/kN
	ϵ_o	$2.65 \cdot 10^{-4}$	m^2/kN
	γ	0.569	–
	m	1.664	–
Plastic potential	ψ_1	4.545	–
	ψ_2	0.770	–

Viscous effects within the pore fluid motion are included by the Darcy permeability coefficient k^F. For the considered sand, $k^F = 2.5 \times 10^{-4}$ m/s is an adequate value.

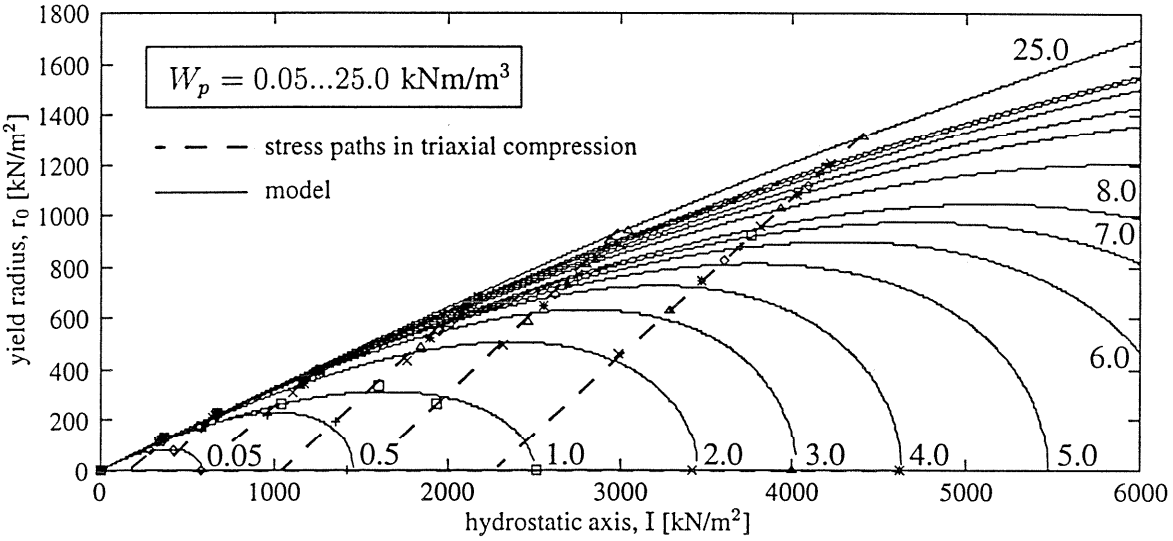

Figure 8. Contours of constant plastic work W_p and experimental data points shown on ($\Theta = 0°$)-plane.

5. FEM CALCULATIONS

The presented elasto-plastic model is implemented in the finite element code PANDAS. For the numerical treatment of the problem, the weak formulation of the field equations (1-3) is used. The incompressibility conditions for both constituents, fluid and solid, lead to a system of differential-algebraic equations (DAE) of first order in time. This DAE system is handled by a diagonally implicit Runge-Kutta (DIRK) time integration scheme (Diebels *et al.* 1998). Time discretization of the elasto-plastic equations, described in Section 3, leads to a system of nonlinear equations. For the solution, a Newton procedure is applied in each time step. A consistent linearization of the nonlinear equations guarantees quadratic convergence within the Newton procedure.

Model validation – triaxial tests:

Predictions for conventional triaxial compression tests on Berlin sand were calculated from the model and compared with experimental results of three similar tests, shown in Figure 9. In these tests, the confining pressure was kept constant at $\sigma_3 = -500$ kN/m^2, while the major principle compressive stress σ_1 was increased up to peak failure. The model predictions capture the observed stress-strain relations accurately.

Coupled solid-fluid problem:

This example handles a fluid-saturated sand region. Load is applied by a time dependent external force on a rigid strip footing. The boundary beside the footing is perfectly drained, the other boundaries are rigid and undrained. Figure 10 shows the contours of isolevels for the effective fluid pressure p at a given time. The arrows display the seepage velocity of the pore fluid. The problem is calculated for different values of the Darcy permeability coefficient k^F.

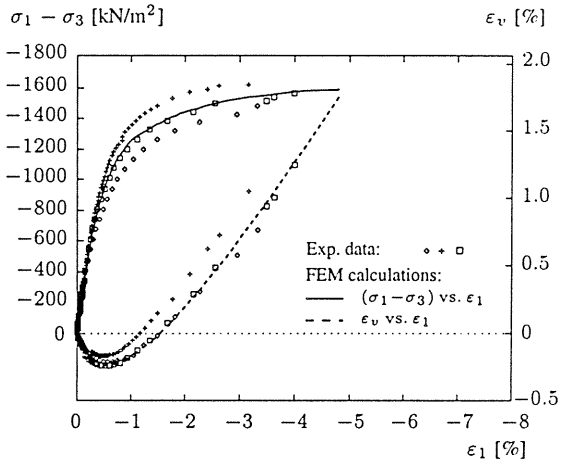

Figure 9. Comparison of FEM calculations with experimental results of conventional triaxial tests ($\sigma_3 = -500$ kN/m^2) on dense Berlin Sand.

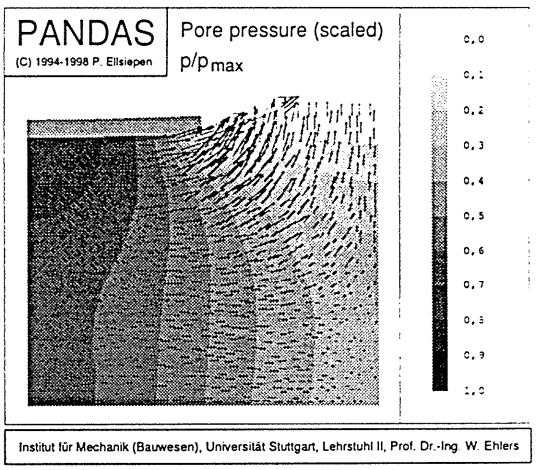

Figure 10. Consolidation of fluid-saturated sand due to foundation loading.

The load is increased linearly at a load-velocity of 1 kN/m^2 per second. The load-settlement and time-settlement curves (Figure 11) demonstrate the influence of the variation of k^F on the displacement of the footing. The viscocity of the fluid leads to a time-dependent deformation. In case of a higher value of k^F, the settlement is larger, since fluid pressure decreases very fast and the soil matrix has to carry the greater part of the load (Figure 11a). In Figure 11b, the load is kept constant at 500 s, after some time the curves converge to the final settlement.

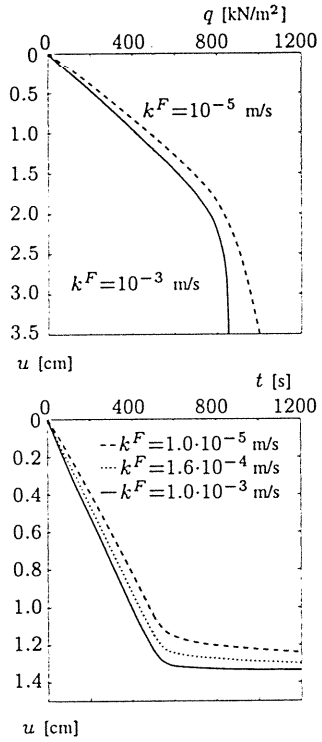

Figure 11. Load-settlement/Time-settlement curves.

6. CONCLUSIONS

In the present article it was shown that a unified approach can be used to describe the stress-strain behaviour of frictional materials. A combination of elasticity and plasticity theories may provide a reasonable and consistent description of this behaviour. In addition to a non-linear elasticity law, the components of this framework are the single-surface yield function, the plastic potential, the flow rule and the work-hardening law.

The elasto-plastic model within a multiphase theory is implemented in the FEM code PANDAS. Validation of the model was achieved by comparison of predicted and experimental stress-strain curves.

As for restriction, the presented model is considered to be only valid as far as unload-reload cycles remain limited. In the unlimited case and in case of cyclic compression-extension tests, the model should be extended by the inclusion of kinematic hardening effects.

REFERENCES

de Boer, R., Ehlers, W., Kowalski, S. and Plischka, J. (1991). *Porous Media – A Survey of Different Approaches*, Forschungsberichte aus dem Fachbereich Bauwesen, Heft 54, Universität-GH-Essen.

de Boer, R. and Ehlers, W. (1990). Uplift, friction and capillarity: Three fundamental effects for liquid-saturated porous solids. *Int. J. Solids Structures*, Vol. 26, No. 1, pp. 43-57.

Bowen, R. M. (1976). *Theory of mixtures*, in A. C. Eringen (ed.): Continuum Physics, Vol. III, Academic Press, New York, pp. 1-127.

Bowen, R. M. (1980). Incompressible porous media models by use of the theory of mixtures, *Int. J. Engng. Sci.*, 18, pp. 1129-1148.

Diebels, S., Ellsiepen, P. and Ehlers, W. (1998). Error-controlled Runge-Kutta Time Integration of a Viscoplastic Hybrid Two-phase Model, *Technische Mechanik*, submitted 4/1998.

Diebels, S., Ellsiepen, P. and Ehlers, W. (1998). *A two phase-model for visco-plastic geomaterials*, Proceedings of the International Symposium on Dynamics of Continua, Bad Honnef 1996, appears in 1998.

Ehlers, W. (1993). *Constitutive equations for granular materials in geomechanical context*, In K. Hutter (ed.): Continuum Mechanics in Environmental Sciences and Geophysics, CISM Courses and Lecture Notes No. 337. Springer-Verlag, Berlin, pp. 313-402.

Ehlers, W. (1995). A single surface yield function for geomaterials, *Arch. Appl. Mech.*, 65, pp. 63-76.

Ehlers, W. and Mahnkopf, D. (1998). Elstoplastizität und Lokalisierung poröser Medien bei finiten Deformationen, *ZAMM 98*, submitted 5/1998.

Lade, P. V. and Kim, M. K. (1988). Single Hardening Constitutive Model for Frictional Materials, Part II, *Computers and Geotechnics*, 6, pp. 13-29.

Loret, B. (1985). On the choice of elastic parameters for sand, *Int. J. Num. Anal. Methods Geomech.*, 9, pp. 285-292.

Terzaghi, K. (1943). *Theoretical Soil Mechanics*, Wiley, New York.

Truesdell, C. and Toupin, R. A. (1960). *The classical field theories*, In S. Flügge (ed.): Handbuch der Physik, Band III/1, Springer-Verlag, Berlin, pp. 226-902.

Yamada, Y. and Ishihara, K. (1979). Anisotropic Deformation Characteristics of Sand under Three Dimensional Stress Conditions, *Soils and Foundations*, JSSMFE, 19, pp. 79-94.